Synthesis and relevant electrochemical properties of 2-hydroxypropyltrimethyl ammonium chloride chitosan-grafted multiwalled carbon nanotubes

Wei Li · Ling Xiao · Caiqin Qin

Abstract The 2-hydroxypropyltrimethyl ammonium chloride chitosan (HACC)-grafted multiwalled carbon nanotubes (MWCNTs) composite (HACC–MWCNTs) was prepared via covalently grafting HACC onto the surfaces of MWCNT. The properties and morphology of the resulting materials were monitored by Fourier transform infrared spectroscopy (FTIR), transmission electron microscopy (TEM), scanning electron microscopy (SEM), and thermogravimetric analysis (TGA). The results of FTIR and TGA indicated that the interaction between MWCNT and HACC was grafting through covalent links. TEM and SEM images confirmed MWCNT stained with an extra phase after the grafting process that was presumed to come from HACC. The dispersion of MWCNT in H_2O was improved after the grafting of HACC, which was in agreement with the positive charge of HACC–MWCNT at any pH value. The electrochemical properties of HACC–MWCNT were investigated by cyclic voltammetry (CV). The dramatic improvement in the electrostatic interactions between HACC–MWCNT/electrode and anionic complexes was distinguished from the response of chitosan-MWCNT/electrode and non-modified electrode. According to the experimental results, the HACC–MWCNT had a possibility to serve as a novel material for innovative anionic sensor.

W. Li · L. Xiao (✉) · C. Qin
Department of Environmental Science, College of Resource and Environmental Science, Wuhan University, 430072 Wuhan, People's Republic of China
e-mail: xiaoling9119@yahoo.cn

C. Qin
Laboratory for Natural Polysaccharides, Xiaogan University, 432000 Xiaogan, People's Republic of China

Introduction

Due to their unique electrical and mechanical properties, carbon nanotubes (CNTs) have received enormous attention for the preparation of electrochemical sensor. Lower overvoltages and higher peak currents were observed in the voltammetric response of several molecules at electrodes modified with CNTs [1–3]. One of the problems for the preparation of these sensors based on CNTs was their insolubility in usual solvents [4, 5]. Therefore, several strategies have been proposed for the immobilization of CNTs on electrochemical transducers, such as dispersion in different solvents or polyelectrolytes and incorporation in composite matrices using distinct binders [2, 5]. Among these dispersing agents, chitosan was the one that offered the best response once cast on the electrode surface (using hydrogen peroxide as marker) [6]. Moreover, chitosan with natural content of hydroxyl and amino groups is suitable for further simple modification and efficient immobilisation of biomolecules under friendly environment [7, 8].

As mentioned above, to stabilize the resulting layer, an additional pretreatment was necessary to perform either in NaOH or in glutaraldehyde after dropping the dispersion on the electrode surface [9–11]. The electrochemical properties of chitosan would be changed because $–NH_2$ and –OH functional groups were reacted in non-covalent [12, 13] or covalent procedures [14, 15]. On the other hand, the positive charge of chitosan–CNTs composites was due to the protonated amine groups within the chitosan matrix at low pH value. The surface charge of the composite was changed with the deprotonation of the $–NH_3^+$ groups [16, 17]. The pH value in the solution was one of the most predominant parameters of the electrostatic interactions which influenced the protonation or deprotonation of the chitosan–CNTs composites [18, 19]. In this article,

we chose 2-hydroxypropyltrimethyl ammonium chloride chitosan (HACC) as a modifier and presented the synthesis of HACC–MWCNTs. Covalent functionalization of WMCNT with HACC could make the resulting composites more stable and controllable [20, 21]. Owing to the –$CH_2CH(OH)CH_2N^+(CH_3)_3Cl$ groups of HACC, the dispersibility of WMCNT would be enhanced. The positively charged HACC–MWCNT could react with negatively charged materials at any pH value as the same mechanism which was proposed for the protonated –NH_2 groups in aqueous acidic solution.

Experimental

Reagents and equipment

The MWCNTs produced by chemical vapor deposition were obtained from Shenzhen Nanotech Port Co (China). The raw nanotubes were 6–10 μm in length. The outer diameter and inner diameter of MWCNT were 20–40 and 10–25 nm, respectively. HACC was obtained by modifying chitosan with 2,3-epoxypropy trimethylammonium chloride according to the literature [20]. The product had a degree of quaternization of 105%. Chitosan–MWCNT was obtained by modifying MWCNT with chitosan according to the literature [14]. All other reagents were commercially available and of analytical grade. All the solutions were prepared with deionized water.

FTIR were recorded on Nicolet Impact 380 spectrophotometer. TGA of the samples were performed on a DuPont Thermal Analyzer 951 under air flow of 100 mL/min, with a heating ramp of 10 °C/min until 700 °C. The samples were kept for 30 min at 100 °C to remove absorbed water. The morphological structures were examined by Hitachi 8000 transmission electron microscope (TEM) and Hitachi S-3200N scanning electron microscope (SEM). The zeta potentials were measured by Malvern Zetasizer Nano ZS. Electrochemical measurements were carried out using a CHI 760A Electrochemical Analyzer. A three-electrode cell (10 mL) with the modified glassy carbon electrode (GCE) as the working electrode, a saturated calomel electrode (SCE) as reference electrode, and a platinum foil electrode as counter electrode was used. The potentials were measured and reported versus the SCE. All measurements were conducted under the presence of a nitrogen atmosphere.

Synthesis of HACC–MWCNT

The general procedure adopted for the preparation of HACC–MWCNT is given in Scheme 1. The pristine MWCNT were immersed into 37% HCl solution with the aid of ultrasonication for 6 h and stayed overnight. The carboxylated MWCNT (MWCNT-COOH) were obtained according to reported method [21]. The MWCNT-COOH were reacted with excess $SOCl_2$ under reflux at 75 °C for 24 h to give acyl chloride-functionalized MWCNT (MWCNT-COCl). After filtration, the residual $SOCl_2$ was removed by the reduced pressure distillation [22]. Then to methylsulfonic acid was added the MWCNT-COCl and HACC, respectively. The mixture was stirred for 24 h at 0 °C under N_2. After reaction, the mixture was filtered and washed with 0.5% acetic acid for three times and then washed with deionized water until pH 7. The product was dried in a vacuum oven.

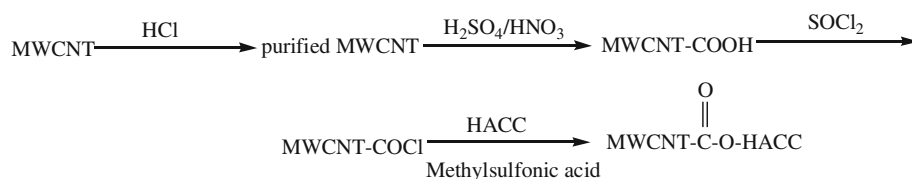### The preparation of electrode modified with HACC–MWCNT

The HACC–MWCNT suspension was prepared by dispersing 5-mg synthetic copolymer into 5-mL deionized water with ultrasonication for about 15 min. A high dispersed colloidal solution was formed. This was very different from the MWCNT that could not disperse effective in water by ultrasonication. A glassy carbon electrode (GCE) (3-mm diameter) was used as the substrate electrode to prepare the modified electrode. The electrode was first polished on finer sandpaper, further polished using alumina slurry (successively 0.5-, 0.1- and 0.05-μm particles), and finally rinsed with deionized water. Then, the electrode was sonicated in 1:1 nitric acid, acetone, and deionized water, respectively [23]. Subsequently, the composite solution was evenly onto a GCE surface with a syringe (10 μL). The modified GCE was further dried under room temperature overnight and was rinsed with deionized water for three times before use.

Results and discussion

The dispersibility of materials

The first indication of successful reaction was increased dispersibility of the HACC–MWCNT, tested by
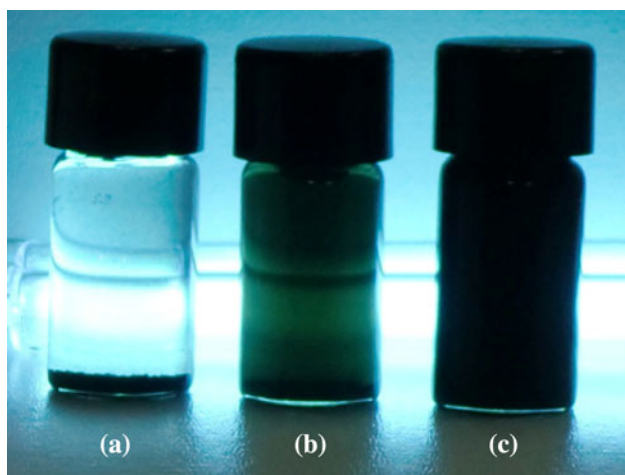
Scheme 1 The functionalization of MWCNT

$$MWCNT \xrightarrow{HCl} purified\ MWCNT \xrightarrow{H_2SO_4/HNO_3} MWCNT\text{-}COOH \xrightarrow{SOCl_2}$$

$$MWCNT\text{-}COCl \xrightarrow[\text{Methylsulfonic acid}]{HACC} MWCNT\text{-}\overset{\overset{\displaystyle O}{\|}}{C}\text{-}O\text{-}HACC$$

Fig. 1 Dispersions of pristine MWCNTs (**a**), carboxylated MWCNT (**b**), and HACC-MWCNT (**c**) after ultrasonicating them in water for 10 min

Fig. 2 Fourier transform infrared spectra of chitosan (*a*) and HACC (*b*)

Fig. 3 Fourier transform infrared spectra of HCl-treated MWCNT (*a*), carboxylated MWCNT (*b*), and HACC-MWCNT (*c*)

ultrasonicating samples in water for 10 min, as compared to the behavior of pristine and carboxylated MWCNT. The pristine MWCNT began to precipitate immediately after ultrasonication (Fig. 1a). The carboxylated MWCNT precipitated slowly, leading to lower transparence of the dispersion (Fig. 1b). Contrastively, the HACC–MWNT dispersion kept their intense coloration for more than 24 h (Fig. 1c). In addition, HACC–MWCNT solution could be homogeneous through the range of pH investigated (pH 1–12). The enhanced dispersion properties were attributed to HACC modified onto the surface of MWCNT which acted as a polymeric cationic surfactant in the solutions [17, 18].

Interaction between HACC and MWCNT

The FTIR spectra of chitosan (Fig. 2a) and HACC (Fig. 2b) were measured with KBr pellets in the range of 500–4000 cm^{-1}. The absorption peak at 1561 cm^{-1} in Fig. 2a ascribed to the N–H bending mode in the primary amine, disappeared in Fig. 2b, suggesting that *N*-alkylation in chitosan occurred. The three intrinsic peaks at 1483, 1640, and 2926 cm^{-1}, which were attributed to the bending mode and flex mode of –CH_3 in quaternized ammonium, respectively, indicated that the proton in the primary amine was substituted by –$CH_2CH(OH)CH_2N^+(CH_3)_3Cl$ [24]. Figure 3b showed the infrared spectrum of carboxylated MWCNT. The peak at 1716 cm^{-1} could be assigned to characteristic of acid carbonyl stretches [25]. The results indicated that carboxylic acid groups had been attached to the surface of MWCNT. The MWCNT with carboxyl acid groups reacted with thionyl chloride and HACC to form HACC–MWCNTs, whose infrared spectrum has been shown in Fig. 3c. Three kinds of peaks were observed at
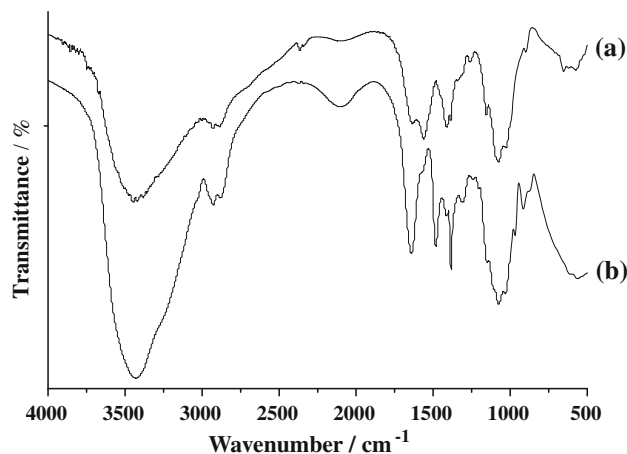
3412 cm^{-1} (the stretch vibration absorption of OH), 1735 cm^{-1} (the stretch vibration absorption of C=O), 1428, 1627, and 2921 cm^{-1} (the antisymmetric and symmetric stretch vibration absorption of CH_3, CH_2, and CH), suggesting the presence of fatty ester [26]. The peaks at 1154 and 1098 cm^{-1} came from the stretch vibration absorption of C–O in ester bond [27, 28]. From the intensity differences of the peaks, it suggested that the –COOH of MWCNT was reacted mainly with the –OH of HACC and formed ester (–COO–) bands.

To further prove the presence of HACC in the synthetic copolymer, TGA were performed to characterize the thermal behavior of the HACC, carboxylated MWCNT, and HACC–MWCNT. It was found that a weight loss due to organics decomposition for HACC–MWCNT was observed in a temperature interval of 260–360 °C (Fig. 4b) [29, 30], then it was more gradual until about 500 °C, becoming sharp again until total decomposition of MWCNT [31]. The content of

Fig. 4 TGA curves of the carboxylated MWCNT (*a*), HACC-MWCNT (*b*), HACC-MWCNT after ultrasonication (*c*), and HACC (*d*)
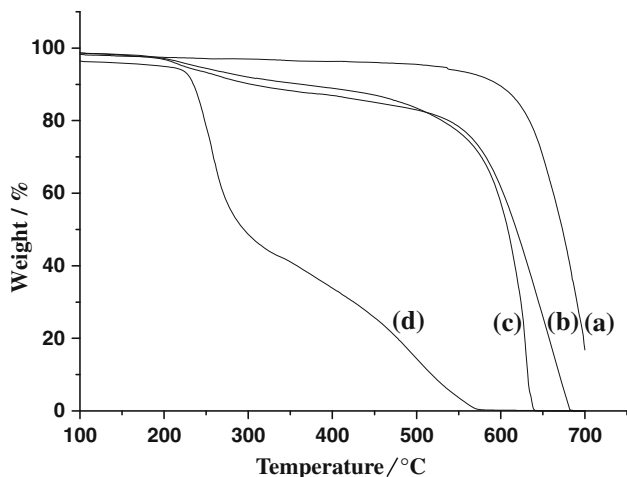

Fig. 5 DTG curves of the carboxylated MWCNT (*a*), HACC-MWCNT (*b*), HACC-MWCNT after ultrasonication (*c*), and HACC (*d*)

organics estimated from the first interval of 260–360 °C was 10.2% for HACC–MWCNT. The high weight loss and the similarity between Fig. 4b and d rise question on possible physical adsorption of HACC to MWCNT. So we dispersed HACC–MWCNT into deionized water with ultrasonication for 30 min to move unbound HACC. The samples in the solution were then filtered and dried under vacuum. The TGA curve of the product is shown in Fig. 4c. The 9.8% weight loss was found in a temperature interval of 260–360 °C and very close to the value in Fig. 4b. If HACC was physically absorbed onto MWCNT, there would have an evident change of weight loss after ultrasonication procedure. In order to examine the thermal behavior of decomposition in detail, differential thermogravimetric (DTG) and differential scanning calorimetry (DSC) curves were obtained. The DTG and DSC curves of HACC (Figs. 5d, 6d) showed two slope change regions at 250–450 °C, while the carboxylated MWCNT (Figs. 5a, 6a) were thermally stable in this temperature region. As shown in Figs. 5 and 6, no significant differences could be observed between the decomposition procedures of HACC–MWCNT and HACC–MWCNT after ultrasonication. There were two exothermal peaks of organics decomposition at 220–450 °C, whose counterpart can be found in the TGA curves. As the temperature of the system exceeded 500 °C, the nanotube samples began to decompose. The nanotubes samples did not fully evaporate until the temperature reaches 650 °C [32, 33]. The structural regularity of a polymer material, contributing to the crystallinity, was also involved in the properties of thermal stability. HACC with linear chains has a well-packed network structure due to the intermolecular H-bonding between –OH groups as well as –NH$_2$ groups. The reaction between HACC and MWCNT may change the regularity of the polymer network, and to some extent,
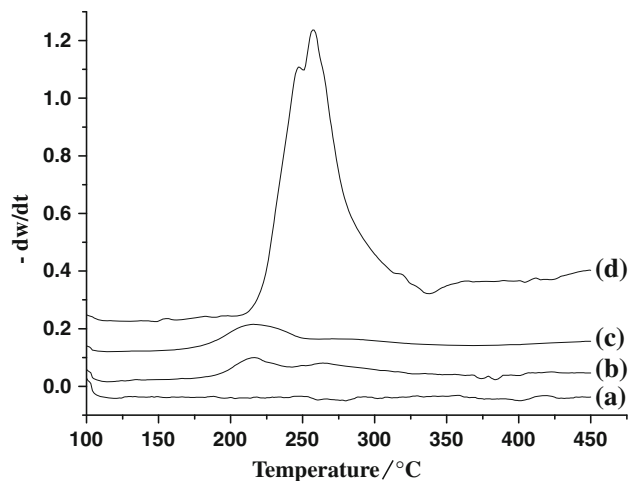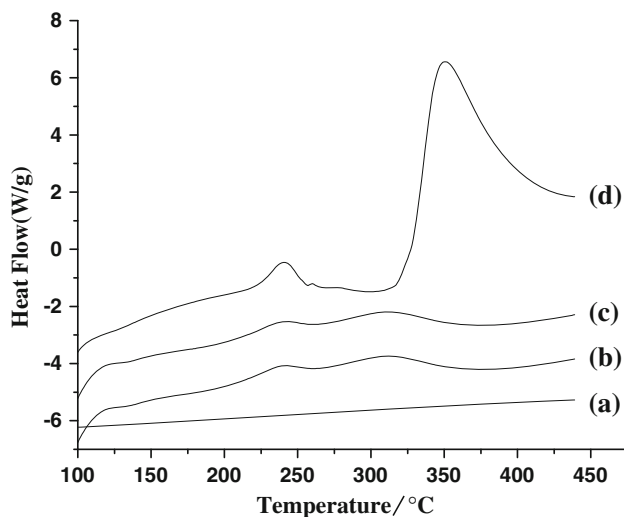

Fig. 6 DSC curves of the carboxylated MWCNT (*a*), HACC-MWCNT (*b*), HACC-MWCNT after ultrasonication (*c*), and HACC (*d*)

decrease the thermal stability [34]. As a result, the initial decomposition temperature of HACC and MWCNT parts in HACC–MWCNT decreased from 250 to 220 °C, and from 550 to 500 °C, respectively.

Transmission electron microscopy (TEM) studies

Transmission electron microscopy was performed to observe the microstructure of carboxylated MWCNT (Fig. 7a, b) and HACC–MWCNT (Fig. 7c, d). For these studies, a drop of the dispersed sample was left to dry out on a commercial carbon coated Cu TEM grid. It appeared that the tips of the MWCNT were opened after acid
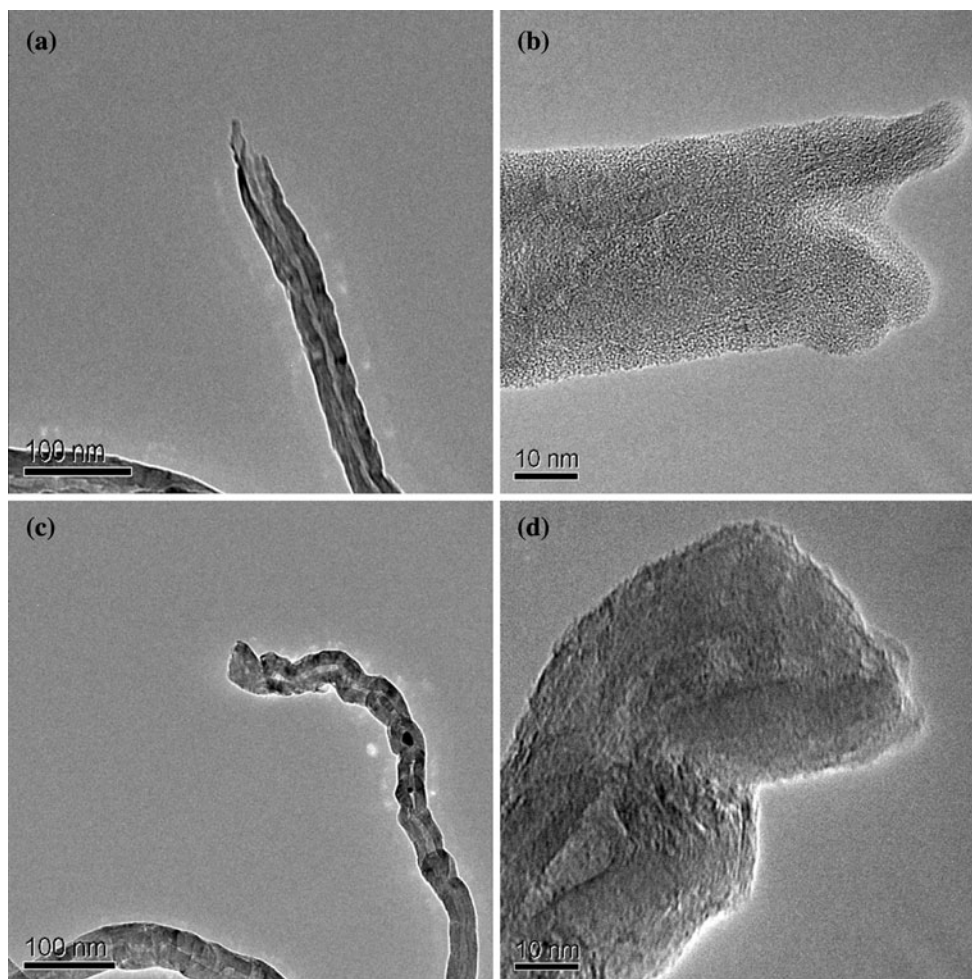
Fig. 7 The TEM images of carboxylated MWCNT (**a**, **b**) and HACC-MWCNT (**c**, **d**)

treatment and resulted in an open-end MWCNT with the removal of the amorphous carbon and metal particles [35]. The carboxylated MWCNT walls were relatively smooth and clean. The HACC–MWCNT appeared stained with an extra phase that was presumed to mainly come from the grafted HACC. Especially at the tips of MWCNT, the core–shell structure of HACC–MWCNT was observed clearly (Fig. 7d).

Relevant electrochemical properties study of HACC–MWCNT

One promising application of HACC–MWCNT was their use in electrochemical sensors. The SEM images of carboxylated MWCNT and HACC–MWCNT were obtained after evaporating a drop of an aqueous suspension of the sample on a glass carbon substrate (Fig. 8). The carboxylated MWCNT walls did not appear covered with any extra phase (Fig. 8a, b). In contrast, it could be seen that the HACC–MWCNT film had many white dots, with

buckles and bends which were consequences of the chemical processing, as shown in Fig. 8c and d. The HACC–MWCNT walls were covered with an extra phase (HACC) which could offer a higher accessible surface area than carboxylated MWCNT. The breakdown of the nanotube structure occurs during the reaction caused by the great number of reaction sites on the tube surface.

The surface charge properties of MWCNT were altered by the functional groups of HACC. Figure 9 showed the zeta-potential curves for HACC–MWCNT (Fig. 9a), chitosan-MWCNT (Fig. 9b), and carboxylated MWCNT (Fig. 9c) in aqueous solution. The zeta-potential values of chitosan-MWCNT decreased with increasing pH and became negative above pH 3.6 that was due to the deprotonation of the $-NH^{3+}$ groups [17–19]. The carboxylated MWCNT was found to be negatively charged in the whole pH range investigated. In contrast, the zeta-potential of HACC–MWCNT is influenced slightly by the solution pH and positively charged at pH values investigated. This change was attributed to the $-CH_2CH(OH)CH_2N^+$

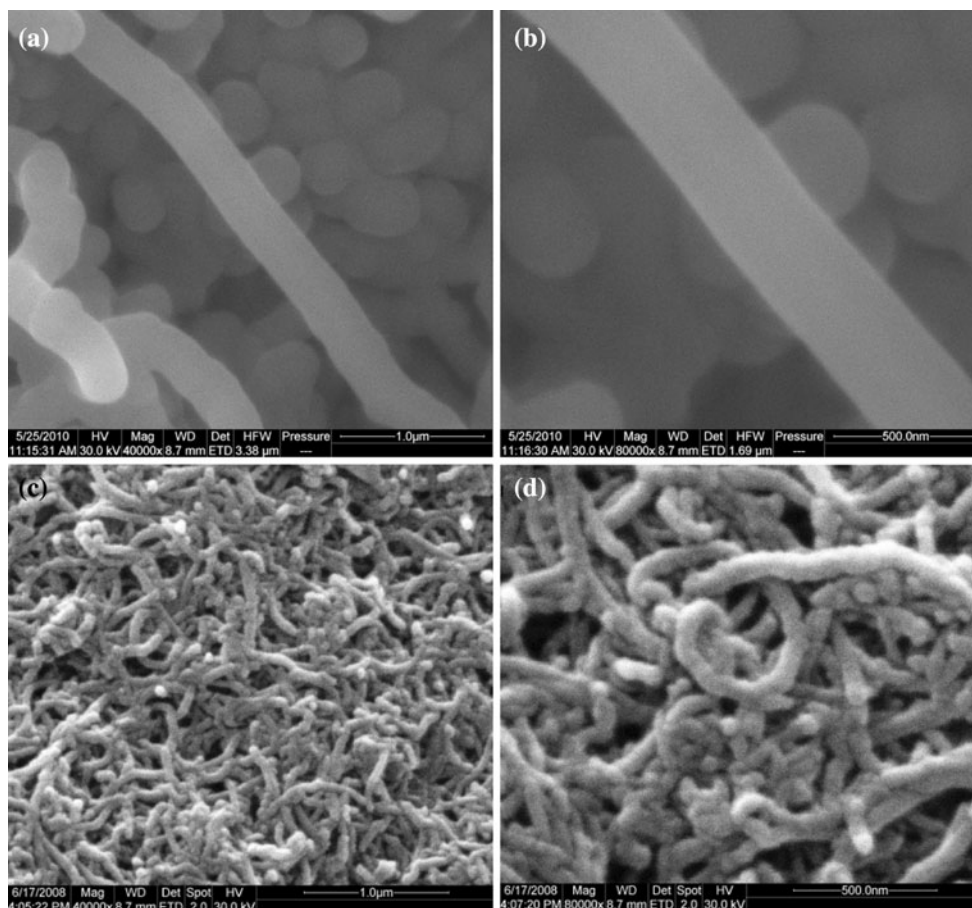**Fig. 8** The SEM images of carboxylated MWCNT (**a**, **b**) and HACC-MWCNT (**c**, **d**)
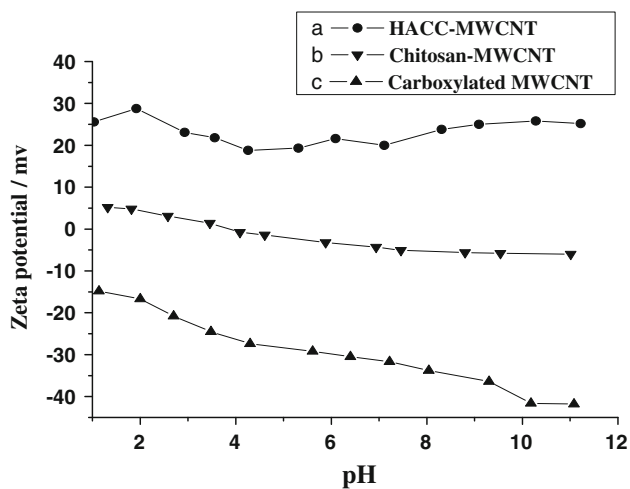

Fig. 9 Dependence of zeta-potential on pH for HACC-MWCNT (*a*), chitosan-MWCNT (*b*), and carboxylated MWCNT (*c*). The samples were measured at 25°C. The pH was changed by adding either HCl or NaOH

$(CH_3)_3Cl$ groups that could not be deprotonated with the change of pH value and make HACC–MWCNT positively charged throughout the range of pH value [36].

The electron transfer between the solution species and the electrode must occur by tunneling either through the barrier or through the defects in the barrier. Therefore, ferricyanide was chosen as a marker to investigate the changes of electrode behavior after modification [37]. The electrochemical activity of the $Fe(CN)_6^{3-/4-}$ redox couple at the HACC–MWCNT-coated glass carbon electrode was probed using cyclic voltammetry between 0.80 and −0.6 V in the presence of 0.1 mM $Fe(CN)_6^{3-/4-}$ in 0.1 M KCl solution. A single CV of $Fe(CN)_6^{3-/4-}$ at the HACC–MWCNT-coated electrode (Fig. 10a) was comparable to that observed at the chitosan-MWCNT-coated electrode (Fig. 10b) and carboxylated MWCNT-coated electrode (Fig. 10c). The HACC–MWCNT-coated electrode exhibited the highest activities towards the reference redox probe, indicating that the process of electron transfer between $Fe(CN)_6^{3-/4-}$ and the electrode was enhanced [38, 39]. After subtracting the background current, the peak current at HACC–MWCNT-coated electrode was three times that at bare electrode and two times that at carboxylated MWCNT-coated electrode. The peak current was directly proportional to the active electrochemical area
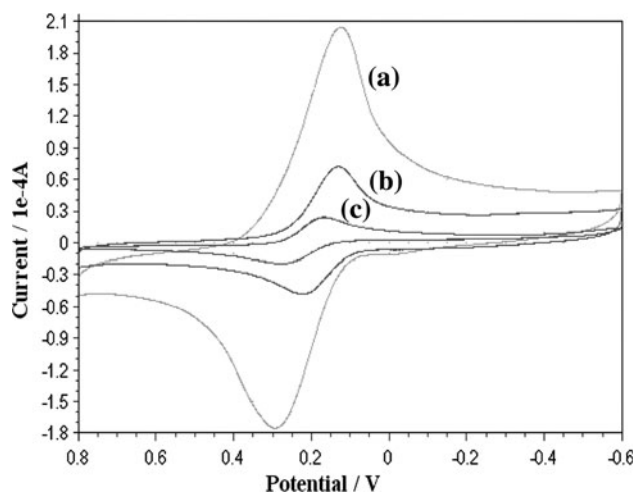
Fig. 10 Cyclic voltammograms (0.01 V/s scan rate) of $Fe(CN)_6^{3-/4-}$ at HACC-MWCNT/GCE (*a*), chitosan-MWCNT/GCE (*b*), and carboxylated MWCNT/GCE (*c*) and in the presence of 0.1 mM $Fe(CN)_6^{3-/4-}$ and 0.1 M KCl solution

[40, 41]. It indicated that the electrochemically active area of MWCNT was increased greatly after grafting HACC.

The peak current increases significantly over time as the HACC–MWCNT-coated electrode was cycled in the $Fe(CN)_6^{3-/4-}$ solution (Fig. 11a). Both cathodic and anodic peak currents gradually increased with subsequent potential scans reaching limiting values after about 40 cycles. It was attributed to electrostatic association of negatively charged $Fe(CN)_6^{3-/4-}$ with quaternized amine groups in the HACC–MWCNT film, resulting in an increase in the concentration of reducible $Fe(CN)_6^{3-/4-}$ near the electrode surface [42]. To examine the extent of association of the $Fe(CN)_6^{3-/4-}$ ions with the HACC–MWCNT film, the electrode was removed from the solution after 40 potential cycles, rinsed briefly with redistilled water, and cycled over the same potential region in supporting electrolyte solution (Fig. 11b). The cathodic and anodic peak currents gradually decay with increasing number of scans. Loosely associated $Fe(CN)_6^{3-/4-}$ ions diffuse out of the chitosan film over time, but there exists a population of $Fe(CN)_6^{3-/4-}$ ions that are strongly associated with the HACC–MWCNT film whose redox signature can be measured over many cycles. The persistent $Fe(CN)_6^{3-/4-}$ signal after repeated cycling in electrolyte solution indicates that residual $Fe(CN)_6^{3-/4-}$ ions are trapped in the HACC–MWCNT film due to electrostatic interactions [43].

Conclusions

In this study, a HACC–MWCNTs was prepared through grafting HACC onto the surfaces of MWCNT. The differences in the FTIR and TGA curves between the
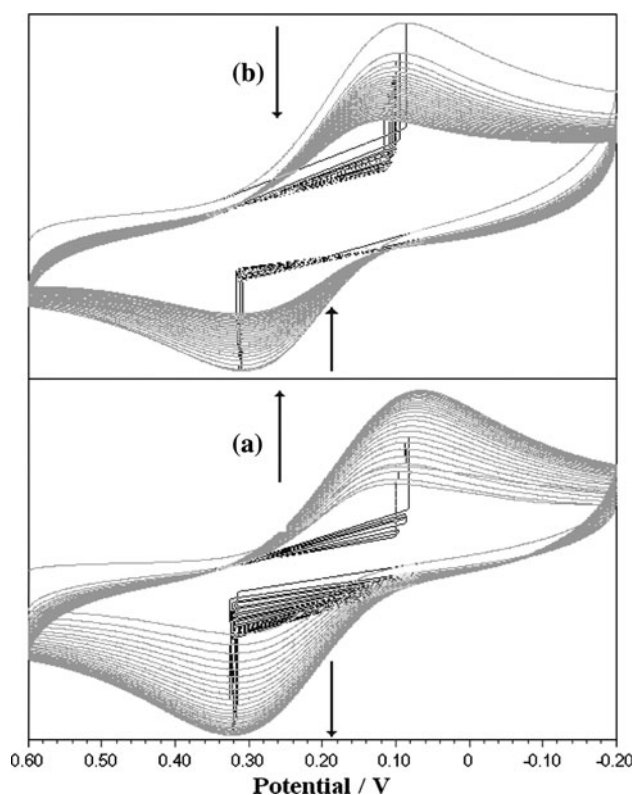

Fig. 11 Cyclic voltammograms (50 cycles at 0.1 V/s scan rate) at HACC-MWCNT/GCE in 0.1 mmol/L $Fe(CN)_6^{3-/4-}$/0.1 mol/L KCl (**a**) and 0.1 mol/L KCl (**b**) solution. *Arrows* show peak progression versus scan cycle

materials indicated the existence of a strong link between HACC and MWCNT in the structure. This result was further confirmed by TEM and SEM images that the shell structure and extra phase of HACC on the surface of MWCNT were observed. A high dispersed colloidal solution was formed easily by dispersing HACC–MWCNT into water with ultrasonication through the range of pH value (1–12). The HACC–MWCNT maintained positive charge at any pH value also. These effects were attributed to the $-CH_2CH(OH)CH_2N^+(CH_3)_3Cl$ groups of HACC. It was very different from chitosan-modified composites whose positive charge was mainly due to protonated amine groups in aqueous acidic solution. The cyclic voltammetry of the negatively charged redox probe, $Fe(CN)_6^{3-/4-}$, showed that the electrochemically active area of MWCNT was increased greatly after grafting HACC. The negatively charged ions were retained in the HACC–MWCNT film by the electrostatic interactions. The retention of negatively charged ions has consequences when used as sensors for the negatively charged molecules. Further application of this material to supercapacitors and sensors are expected and currently under investigation.

References

1. Merkoçi A, Pumera M, Llopis X, Pérez B, Valle M, Alegret S (2005) Trends Anal Chem 24(9):826
2. Coleman JN, Khan U, Blau WJ, Gun'ko YK (2006) Carbon 44:1624
3. Carrara S, Shumyantseva VV, Archakov AI, Samor B (2008) Biosens Bioelectron 24:148
4. Buratti S, Brunetti B, Mannino S (2008) Talanta 76:454
5. Shobha Jeykumari DR, Ramaprabhu S, Sriman Narayanan S (2007) Carbon 45:1340
6. Wei C, Srivastava D, Cho K (2004) Nano Lett 4:1949
7. Wang J, Kawde A-N, Jan MR (2004) Biosens Bioelectron 20:995
8. Yogeswaran U, Chen S-M (2008) Sens Actuators B 130:739
9. Guibal E (2005) Prog Polym Sci 30:71
10. Chiou MS, Li HY (2003) Chemosphere 50:1095
11. Binsu VV, Nagarale RK, Shahi VK, Ghosh PK (2006) React Funct Polym 66:1619
12. Tkac J, Whittaker JW, Ruzgas T (2007) Biosens Bioelectron 22:1820
13. Liu Y, Tang J, Chen X, Xin JH (2005) Carbon 43:3178
14. Wu Z, Feng W, Feng Y, Liu Q, Xu X, Sekino T et al (2007) Carbon 45:1212
15. Kong H, Gao C, Yan D (2004) J Am Chem Soc 126(2):412
16. de Moura MR, Aouada FA, Mattoso LHC (2008) J Colloid Interface Sci 321:477
17. Anal AK, Tobiassen A, Flanagan J, Singh H (2008) Colloids Surf B 64:104
18. Jansson-Charrier M, Guibal E, Roussy J, Delanghe B, Le Cloirec P (1996) Water Res 30(2):465
19. Dzul Erosa MS, Saucedo Medina TI, Avarro Mendoza R, Avila Rodriguez M, Uibal E (2001) Hydrometallurgy 61:157
20. Loubaki E, Ourevitch M, Sicsic S (1991) Eur Polym J 27(3):311
21. Shieh Y-T, Yang Y-F (2006) Eur Polym J 42:3162
22. Shen J, Huang W, Wu L, Hua Y, Ye M (2007) Mater Sci Eng A 464:151
23. Yao H, Li N, Xu J-Z, Zhu J-J (2007) Talanta 71:550
24. Huang R, Chen G, Sun M, Hu Y, Gao C (2006) J Membr Sci 286:237
25. Xiong J, Zheng Z, Qin X (2006) Carbon 44:2701
26. Miao Z, Yang J, Wang L (2008) Mater Lett 62:3450
27. Zheng Z, He P-J, Shao L-M (2007) Water Res 41:4696
28. Oki A, Adams L, Khabashesku V (2008) Mater Lett 62:918
29. Chen E-C, Wu T-M (2007) Polym Degrad Stab 92:1009
30. Li J, Tong L, Fang Z (2006) Polym Degrad Stab 91:2046
31. Bikiaris D, Vassiliou A, Chrissafis K, Paraskevopoulos KM, Jannakoudakis A, Docoslis A (2008) Polym Degrad Stab 93:952
32. Kweon HY, Um IC, Park YH (2001) Polymer 42:6651
33. Zohuriaan MJ, Shokrolahi F (2004) Polym Test 23:575
34. Ko C-J, Lee C-Y, Ko F-H, Chen H-L, Chu T-C (2004) Microelectron Eng 73–74:570
35. Chen C-M, Chen M, Peng Y-W, Lin C-H, Chang L-W, Chen C-F (2005) Diamond Relat Mater 14:798
36. Zhang J, Wang Q, Wang L, Wang A (2007) Carbon 45:1911
37. Liang R, Peng H, Qiu J (2008) J Colloid Interface Sci 320:125
38. Ojani R, Raoof J-B, Zarei E (2006) Electrochim Acta 52:753
39. Emery SB, Hubbley JL, Roy D (2005) Electrochim Acta 50:5659
40. Trasatti S, Petrii OA (1992) J Electroanal Chem 327:353
41. Xiang C, Zou Y, Suna L-X, Xua F (2006) Electrochim Acta 51:5324
42. Huang R, Chen G, Yang B, Gao C (2008) Sep Purif Technol 61:424
43. Zangmeister RA, Park JJ, Rubloff GW, Tarlov MJ (2006) Electrochim Acta 51:5324